phys. stat. sol. (b) **229**, No. 3, 1427–1449 (2002)

Van Hove Singularity and Superconductivity in a Disordered Hubbard Model

G. LITAK

Department of Mechanics, Technical University of Lublin, Nadbystrzycka 36, PL 20-618 Lublin, Poland

(Received June 27, 2001; in revised form October 5, 2001; accepted October 29, 2001)

Subject classification: 74.20.–z; 74.62.Dh

We apply the Coherent Potential Approximation (CPA) to a simple extended Hubbard model with a nearest and next nearest neighbour hopping for disordered superconductors with s-, d- and p-wave pairing. We show how the Van Hove singularities in the electron density of states enhance the transition temperature T_c for exotic superconductors in a clean and weakly disordered system. The Anderson theorem and the pair-breaking effects in presence of the Van Hove singularity caused by non-magnetic disorder are also discussed.

1. Introduction

Magnetic and non-magnetic impurities in superconductors always attracted interest and their treatment played the essential role in theories of superconductivity.

Since the works of Anderson [1] and Abrikosov and Gorkov [2] the influence of magnetic and non-magnetic disorder on superconductors has been treated in many ways [3–9]. Their arguments, originally applied to classic BCS superconductors, were reexamined for novel, exotic superconductors [10, 11] with the anisotropic order parameters extended s-wave, d-wave character [4, 12–27] and also recently discovered [28–31] p-wave ruthenates [5, 32–35].

Examining the influence of various kinds of magnetic and non-magnetic disorder, caused by structural, substitutional, irradiational defects etc., on properties of conventional and unconventional superconductors has shown, that their responses to disorder are quite different. In contrast to conventional materials where only magnetic impurities affect the superconducting properties, for unconventional superconductors the effect of both magnetic and non-magnetic disorder is usually strong [36–51].

Thus it is not surprising, that the response to disorder becomes the fundamental criterion of unconventionality of the physical mechanism leading to superconductivity. Moreover, effects of disorder are of interest because the high temperature superconductors have to be doped ($La_{2-x}Sr_xCuO_4$ with strontium $x = 0.15$, $YBa_2Cu_3O_{7-x}$ with oxygen $x = 0.1$) to show the optimal critical temperature and doping is always accompanied by disorder.

On the other hand in these quasi two-dimensional layered materials the Fermi energy has been found in the vicinity of Van Hove singularities of the electron density of states [52–67]. This has lead to the formulation of the Van Hove scenario for high temperature superconductors which says that the optimal critical temperature is reached when the chemical potential passes through the Van Hove singularity in the density of states [19, 52, 53, 58]. Doping with charge carriers does not only change the density in the system but also smears the density of states eliminating its singularities

 0370-1972/02/22902-1427 $ 17.50+.50/0

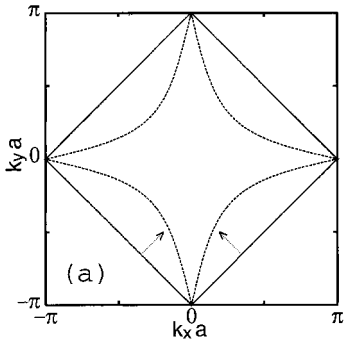

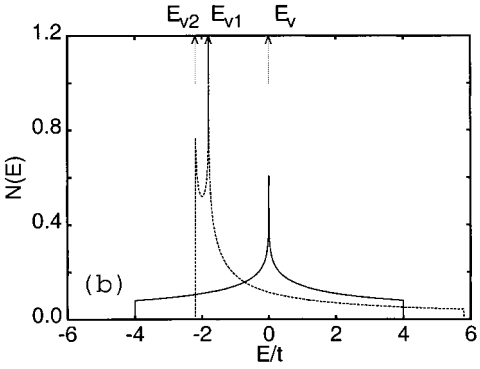

Fig. 1. a) Distortion of the Fermi surface by the next neighbour electron hopping t'. The full line denotes the Fermi surface for $t' = 0$ while the dashed line shows $t' = 0.45t$. Fermi energy is at Van Hove singularity $E_F = E_v$. b) The electron density of states $N(E)$ for the 2D lattice, where the full line corresponds to $t' = 0$ and the dashed line to $t' = 0.45t$. The arrows denote the Van Hove singularities E_v, E_{v1} and E_{v2}, respectively ($E_F = 0$)

and, specially for anisotropic superconductors, introduces the electron pair-breaking phenomenon [4, 6, 12, 20].

Thus one has to investigate the effect of rise and fall of the critical temperature T_c near the Van Hove singularities very carefully simultaneously, taking into account the effects of disorder. Clearly disorder reduces the critical temperature T_c by elimination of singularities in the density of states and, at the same time, by braking pairs. The present paper is the extension of the previous ones [19, 20, 34] where the electron hopping was introduced only between nearest neighbour lattice sites. Here following Refs. [68, 69] we introduce the hopping to the next nearest sites t' (i.e. the ratio of hopping parameters t, t' for YBaCuO was suggested to be $t'/t = 0.45$) and investigate the effect of disorder on superconducting properties.

In the normal states the nonzero hopping to the next neighbour sites t' introduces the distortion of the Fermi surface (Fig. 1a) which results in considerable changes in the electron density of states (Fig. 1b). Note, that in the case $t' \neq 0$ the central Van Hove singularity produces a stronger enhancement of the density of states ($N(E)$ for $E \approx E_{v1}$) than for $t' = 0$ (Fig. 1b). Moreover, the other Van Hove singularity associated with the bottom edge of the band E_{v2} creates the second peak in the density of states $N(E)$. Thus, depending on the band filling, the additional electron hopping t' should have an effect on the critical temperature T_c, rising it to a higher value. On the other hand, the distorted Fermi surface with the stronger dependence on $\mathbf{k}$ (Fig. 1a) seems to be less stable in the presence disorder as $\mathbf{k}$ is not a good quantum number in a disordered system.

The present paper is organized as follows. In Section 2 the discussion starts with the extended attractive Hubbard model defined on the square lattice which has the extended s-, d- and p-wave order parameter solutions. Than we shortly overview and classify various types of Van Hove singularities in the electron density of states of one band model and their influence on the superconducting critical temperature T_c. In Section 3 we investigate disordered superconducting systems and apply the Coherent Po-

tential Approximation (CPA) on the attractive Hubbard model. The Anderson theorem for non-magnetic impurity effect on isotropic s-wave solutions and the pair-breaking effect in case of anisotropic pairing is also discussed. Section 4 is devoted to the examination of the disorder effect on the superconducting critical temperature T_c. Finally, Section 5 contains conclusions and remarks.

2. The Role of Van Hove Singularities in a Clean System

2.1 Bogolyubov-de Gennes equation

We start with the single band Hubbard model with an attractive extended interaction which is described by the Hamiltonian [68–70]

$$H = \sum_{ij\sigma} t_{ij} c^{\dagger}_{i\sigma} c_{j\sigma} + \tfrac{1}{2} \sum_{ij} U_{ij} n_i n_j - \sum_{i} (\mu - \varepsilon_i)\, n_i \,. \tag{1}$$

In the equation above $n_i = n_{i\uparrow} + n_{i\downarrow}$ is the charge on the site labeled i, μ is the chemical potential. Disorder is introduced into the problem by allowing the local site energy ε_i to vary randomly from site to site, $c^{\dagger}_{i\sigma}$ and $c_{i\sigma}$ are the Fermion creation and annihilation operators for an electron on the site i with the spin σ, t_{ij} is the amplitude for hopping from site j to site i (with $t_{ii} = 0$) and finally U_{ij} is the attractive interaction ($U_{ij} < 0$) which causes superconductivity and can be either local ($i = j$) or non-local ($i \neq j$). Starting from Eq. (1) we apply the Hartree-Fock-Gorkov [71] approximation, which results in the Bogolyubov-de Gennes equation for a singlet (s- or d-wave) superconductor:

$$\sum_{l} \begin{pmatrix} (\varepsilon_i - \mu)\,\delta_{il} - t_{il} & -\Delta_{il} \\ -\Delta^{*}_{il} & (-\varepsilon_i + \mu)\,\delta_{il} + t_{il} \end{pmatrix} \begin{pmatrix} u_{l\uparrow} \\ v_{l\downarrow} \end{pmatrix} = E \begin{pmatrix} u_{i\uparrow} \\ v_{i\downarrow} \end{pmatrix}, \tag{2}$$

where $u_{l\uparrow}$ and $v_{l\downarrow}$ are electron and hole wave functions with up anti parallel spins $\uparrow$ and $\downarrow$ respectively. The usual singlet one particle Green function, in the Nambu space $\mathbf{G}(i, j; \mathrm{i}\omega_n)$, at the Matsubara frequency $\omega_n = \dfrac{\pi}{\beta}(2n+1)$ satisfies

$$\sum_{l} \begin{pmatrix} (\mathrm{i}\omega_n - \varepsilon_i + \mu)\,\delta_{il} + t_{il} & \Delta_{il} \\ \Delta^{*}_{il} & (\mathrm{i}\omega_n + \varepsilon_i - \mu)\,\delta_{il} - t_{il} \end{pmatrix} \begin{pmatrix} G_{11}(l, j; \mathrm{i}\omega_n) & G_{12}(l, j; \mathrm{i}\omega_n) \\ G_{21}(l, j; \mathrm{i}\omega_n) & G_{22}(l, j; \mathrm{i}\omega_n) \end{pmatrix} = \delta_{ij}\mathbf{1} \tag{3}$$

where the pairing potentials Δ_{ij} will be taken to be nonzero only when the sites i and j coincide ($i = j$) for on-site interaction U_{ii}, or are nearest neighbours for off-diagonal interaction U_{ij}. On the other hand in case of triplet (p-wave) pairing we have instead of Eq. (2)

$$\sum_{l} \begin{pmatrix} (\varepsilon_i - \mu)\,\delta_{il} - t_{il} & 0 & -\Delta^{\uparrow\uparrow}_{il} & -\Delta^{\uparrow\downarrow}_{il} \\ 0 & (\varepsilon_i - \mu)\,\delta_{il} - t_{il} & -\Delta^{\downarrow\uparrow}_{il} & -\Delta^{\downarrow\downarrow}_{il} \\ -\Delta^{\uparrow\uparrow *}_{il} & -\Delta^{\downarrow\uparrow *}_{il} & (-\varepsilon_i + \mu)\,\delta_{il} + t_{il} & 0 \\ -\Delta^{\uparrow\downarrow *}_{il} & -\Delta^{\downarrow\downarrow *}_{il} & 0 & (-\varepsilon_i + \mu)\,\delta_{il} + t_{il} \end{pmatrix} \begin{pmatrix} u_{l\uparrow} \\ u_{l\downarrow} \\ v_{l\uparrow} \\ v_{l\downarrow} \end{pmatrix} = E \begin{pmatrix} u_{i\uparrow} \\ u_{i\downarrow} \\ v_{i\uparrow} \\ v_{i\downarrow} \end{pmatrix}, \tag{4}$$

rewritten as

$$\sum_{l} \begin{pmatrix} [(\mathrm{i}\omega_n - \varepsilon_i + \mu)\,\delta_{il} + t_{il}]\,\mathbf{1} & \boldsymbol{\Delta}_{il} \\ \boldsymbol{\Delta}^{+}_{il} & [(\mathrm{i}\omega_n + \varepsilon_i - \mu)\,\delta_{il} - t_{il}]\,\mathbf{1} \end{pmatrix} \begin{pmatrix} \mathbf{G}_{11}(l, j; \mathrm{i}\omega_n) & \mathbf{G}_{12}(l, j; \mathrm{i}\omega_n) \\ \mathbf{G}_{21}(l, j; \mathrm{i}\omega_n) & \mathbf{G}_{22}(l, j; \mathrm{i}\omega_n) \end{pmatrix} = \delta_{ij}\mathbf{1} \tag{5}$$

on the analogy of the equation of motion for the Green function in Eq. 3 with the spin dependent 4×4 Green function. Each of its components $\mathbf{G}_{nm}(l,j;\mathrm{i}\omega_n)$ is defined as

$$\mathbf{G}_{nm}(l,j;\mathrm{i}\omega_\nu) = \begin{pmatrix} G^{\uparrow\uparrow}_{nm}(l,j;\mathrm{i}\omega_\nu) & G^{\uparrow\downarrow}_{nm}(l,j;\mathrm{i}\omega_\nu) \\ G^{\downarrow\uparrow}_{nm}(l,j;\mathrm{i}\omega_\nu) & G^{\downarrow\downarrow}_{nm}(l,j;\mathrm{i}\omega_\nu) \end{pmatrix}, \qquad n,m = 1,2\,. \tag{6}$$

The order parameter for triplet pairing reads

$$\mathbf{\Delta}_{ij} = \begin{pmatrix} \Delta^{\uparrow\uparrow}_{ij} & \Delta^{\uparrow\downarrow}_{ij} \\ \Delta^{\downarrow\uparrow}_{ij} & \Delta^{\downarrow\downarrow}_{ij} \end{pmatrix}. \tag{7}$$

We assume that the hopping integrals t_{ij} can take nonzero values for the nearest and next nearest neighbours. For a clean system t_{ij} can be expressed in $\mathbf{k}$-space by the Fourier transform $\epsilon_{\mathbf{k}} = \sum_j t_{ij}\, \mathrm{e}^{-\mathrm{i}\mathbf{R}_{ij}\mathbf{k}}$ as

$$\epsilon_{\mathbf{k}} = -2t(\cos k_x a + \cos k_y a) + 4t' \cos k_x a \cos k_y a\,, \tag{8}$$

where t represents the nearest neighbour site amplitude of electron hopping, while t' corresponds to next nearest neighbour hopping, a denotes the lattice constant, μ is the chemical potential equal to the Fermi energy at zero temperature ($\mu = E_{\mathrm{F}}$ for $T = 0$). We shall refer to the Greens function matrix as $\mathbf{G}(i,j;\mathrm{i}\omega_n)$ which will be of 2×2 or 4×4 size for singlet or triplet solution. The above equations have to be completed by the self-consistency condition for pairing potential

$$\Delta_{ij} = U_{ij} \frac{1}{\beta} \sum_n \mathrm{e}^{\mathrm{i}\omega_n \eta}\, G_{12}(i,j;\mathrm{i}\omega_n)\,, \tag{9}$$

for the singlet pairing case and

$$\Delta^{\alpha\alpha'}_{ij} = U_{ij} \frac{1}{\beta} \sum_n \mathrm{e}^{\mathrm{i}\omega_n \eta}\, G^{\alpha\alpha'}_{12}(i,j;\mathrm{i}\omega_n)\,, \qquad \alpha,\alpha' = \uparrow,\downarrow \tag{10}$$

for the triplet one, where η is a positive infinitesimal, $\beta = \dfrac{1}{Tk_{\mathrm{B}}}$ is the inverse of temperature T and Boltzman constant k_{B} (in the units we use here $k_{\mathrm{B}} = 1$). To simplify matters we have assumed that the Hartree term $U_{ij}\langle n_{j-\sigma}\rangle$ can be absorbed into the hopping integral t_{ij} and dropped it from Eqs. (2) to (5). As usual Eqs. (9) and (10) are to be solved together with the corresponding equations for the chemical potential μ that satisfies

$$n = \frac{2}{\beta} \sum_n \mathrm{e}^{\mathrm{i}\omega_n \eta}\, G_{11}(i,i;\mathrm{i}\omega_n) \tag{11}$$

for singlets or

$$n = \frac{2}{\beta} \sum_n \mathrm{e}^{\mathrm{i}\omega_n \eta}\, G^{\uparrow\uparrow}_{11}(i,i;\mathrm{i}\omega_n) \tag{12}$$

for triplets, where n is the number of electrons per unit cell.

Here we do not wish to be very specific about the physical nature of the point defects represented by the site energies ε_i. We are rather going to provide a reliable analysis of the simplest possible nontrivial model. Thus we take them to be independent random variables defined to have values $\frac{1}{2}\delta$ and $-\frac{1}{2}\delta$ with equal probability of 1/2 on every site [19, 20]. As might be expected we shall be interested in the average of

$\mathbf{G}(i,j;\mathrm{i}\omega_n)$ over the above ensemble. To calculate $\bar{\mathbf{G}}(i,j;\mathrm{i}\omega_n)$ we shall make use of the Coherent Potential Approximation (CPA) which is the best method at hand for the mean field theory of disorder [72].

2.2 Van Hove singularities in clean superconductors

Let us assume that the sites form a square lattice. Then for a clean system ($\varepsilon_i = 0$ for all i), in the normal state, where $\Delta_{ij} = 0$, the spectrum is given by $\epsilon_{\mathbf{k}}$ (Eq. 8). It has a saddle point Van Hove singularity at $E_\mathrm{v} = 4t'$, resulting in the logarithmic divergence of the density of states $N(E) \sim -\ln(E - E'_\mathrm{v})$ (Fig. 1b). The density of states for a normal state $N(E)$ is defined as

$$N(E) = \frac{1}{N}\sum_{\mathbf{k}} \delta(E - \epsilon_{\mathbf{k}}) = \frac{a^2}{4\pi^2} \int\limits_{E=\epsilon_{\mathbf{k}}} \mathrm{d}f\, |\nabla_{\mathbf{k}}\epsilon_{\mathbf{k}}|^{-1}\,, \tag{13}$$

where $\mathrm{d}f$ is an element of the Fermi surface (Fig. 2b). $N(E)$ reaches its maximum if the Fermi surface satisfies the relation $E - \epsilon_{\mathbf{k}} = 0$. Finally, the density of states $N(E)$ can also be expressed by the elliptic function of the first kind $\mathrm{K}(E)$ [65],

$$N(E) = \frac{1}{N}\sum_{\mathbf{k}} \mathrm{Im}\,\frac{1}{E + \mathrm{i}\eta - \epsilon_{\mathbf{k}}} = \frac{1}{2\pi^2 t\,\sqrt{1 + \frac{Et'}{t^2}}}\,\mathrm{K}\left(\sqrt{\frac{16t^2 - (E - 4t')^2}{16t^2(1 + \frac{Et'}{t^2})}}\right). \tag{14}$$

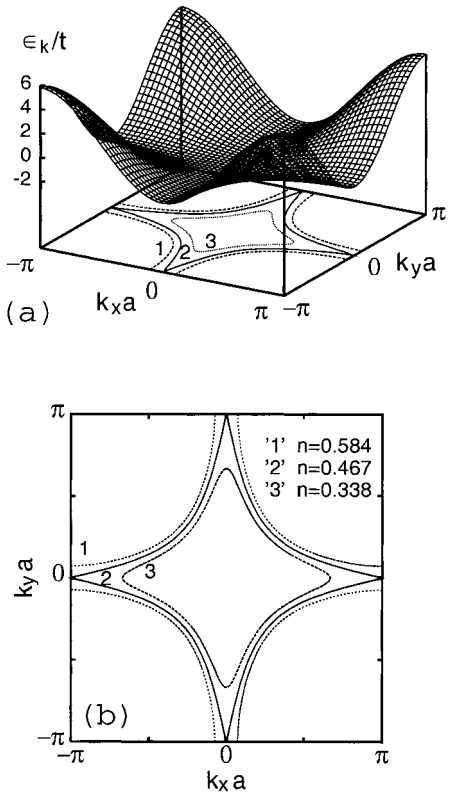

Van Hove singularities in the density of states (Eqs. (13), (14)) correspond to three characteristic flat regions of $\epsilon_{\mathbf{k}}$, where $\nabla_{\mathbf{k}}\epsilon_{\mathbf{k}} = 0$. In Fig. 2a we have plotted band the energy $\epsilon_{\mathbf{k}}$ (Eq. (8)). For cuprates the value of the next nearest neighbour hopping term t' is usually considered as $0 < t' < 0.5t$. Here we have chosen $t' = 0.45t$ (Eq. (8)). One can easily determine Van Hove singularities for saddle points: $(|k_x|, |k_y|) = (\pi/a, 0)$, $(0, \pi/a)$ and these are corresponding to the band edges: the bottom one $(0,0)$ as well as the top one $(\pi/a, \pi/a)$. Three isoenergetic contours '3', '2', '1' have been marked in Fig. 2a for $E/t = 2$, 1.8, 1.6. They correspond to Fermi surfaces (Fig. 2b) for three values

Fig. 2. Band structure (a) and Fermi surfaces (a, b) for the one band electron structure with next nearest neighbour hopping: $\epsilon_{\mathbf{k}} = -2t(\cos k_x + \cos k_y) + 4t' \cos k_x \cos k_y$ with $t' = 0.45t$, and three different band fillings: $n = 0.584$ (1), $n = 0.467$ (2), $n = 0.388$ (3)

of band filling $n = 0.338$, 0.467, 0.584 respectively. Note that for $n = 0.584$ the Fermi surface has hole like characteristics, while for $n = 0.388$ it corresponds to an electron like system. For $n = 0.467$ the Fermi energy $E_F = 1.8t$ passes through the Van Hove saddle point singularity.

For the on-site attraction (negative U) $U_{ii} = U$ the linearized gap equation (Eq. (9)) at T_c can be written as

$$1 = \frac{U}{\pi} \int_{-\infty}^{\infty} \mathrm{d}E \, \frac{1}{N} \sum_{\mathbf{k}} \frac{\delta(E - \epsilon_{\mathbf{k}} - \mu)}{2E} \tanh\left(\frac{\beta_c E}{2}\right) = \frac{U}{\pi} \int_{-\infty}^{\infty} \mathrm{d}E \, \frac{N(E)}{2E} \tanh\left(\frac{\beta_c E}{2}\right), \tag{15}$$

where $\beta_c = 1/(T_c k_B)$, and T_c is a critical temperature.

If the interaction is off-diagonal then the Fourier transform of U_{ij} leads to the expression

$$U(\mathbf{k} - \mathbf{q}) = -|U| \left(\frac{\eta_{\mathbf{k}} \eta_{\mathbf{q}} + \gamma_{\mathbf{k}} \gamma_{\mathbf{q}}}{4} + 2 \sin k_x a \sin q_x a + 2 \sin k_y a \sin q_y a \right), \tag{16}$$

where

$$\begin{aligned} \gamma_{\mathbf{k}} &= 2(\cos k_x a + \cos k_y a), \\ \eta_{\mathbf{k}} &= 2(\cos k_x a - \cos k_y a). \end{aligned} \tag{17}$$

The pairing parameters for the corresponding symmetry of the solution, extended s-, d- or p-wave have the form

$$\begin{aligned} \Delta_{\mathbf{k}}^{\mathrm{s}} &= \Delta_0 \gamma_{\mathbf{k}}, \\ \Delta_{\mathbf{k}}^{\mathrm{d}} &= \Delta_0 \eta_{\mathbf{k}}, \\ \mathbf{\Delta}_{\mathbf{k}}^{\mathrm{p}} &= \mathbf{\Delta}_0^x \sin(k_x a) + \mathbf{\Delta}_0^y \sin(k_y a), \end{aligned} \tag{18}$$

and $\mathbf{\Delta}_{\mathbf{k}}^{\mathrm{p}}$ is a Fourier transform of the matrix $\mathbf{\Delta}_{ij}$ (Eq. (7)). Despite of the different types of possible solutions described by Eqs. (3), (5), (18) the linearized gap equation for the critical temperature can be written in a compact form

$$1 = \frac{U}{\pi} \int_{-\infty}^{\infty} \mathrm{d}E \, \frac{N_\alpha(E)}{2E} \tanh\left(\frac{\beta_c E}{2}\right), \tag{19}$$

depending on the solution symmetry $\alpha = \mathrm{s}, \mathrm{d}, \mathrm{p}$.

The normal density of states $N(E) = \frac{1}{N} \sum_{\mathbf{k}} \delta(E - \epsilon_{\mathbf{k}})$ and the corresponding projected densities ($N_s(E)$, $N_d(E)$ and $N_p(E)$) used in Eq. (19) can be expressed in terms of Green functions of the normal system

$$\begin{aligned} N(E) &= -\frac{1}{N} \sum_{\mathbf{k}} \frac{1}{\pi} \operatorname{Im} G_{11}(\mathbf{k}, E), \\ N_{\mathrm{s}}(E) &= -\frac{1}{N} \sum_{\mathbf{k}} \frac{\gamma_{\mathbf{k}}^2}{4} \frac{1}{\pi} \operatorname{Im} G_{11}(\mathbf{k}, E), \\ N_{\mathrm{d}}(E) &= -\frac{1}{N} \sum_{\mathbf{k}} \frac{\eta_{\mathbf{k}}^2}{4} \frac{1}{\pi} \operatorname{Im} G_{11}(\mathbf{k}, E), \\ N_{\mathrm{p}}(E) &= -\frac{1}{N} \sum_{\mathbf{k}} 2(\sin k_x a)^2 \frac{1}{\pi} \operatorname{Im} G_{11}(\mathbf{k}, E). \end{aligned} \tag{20}$$

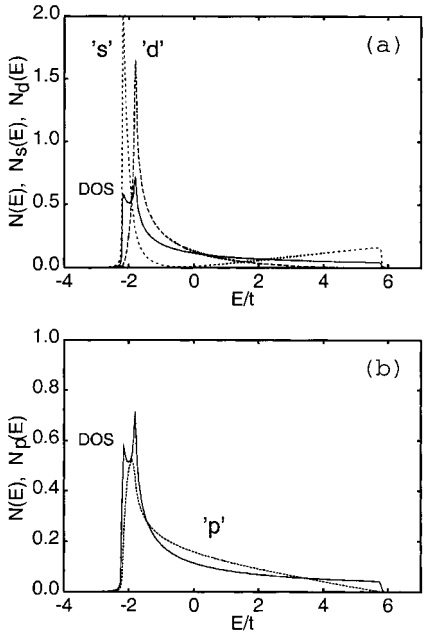

Fig. 3. a) Electron density of states $N(E)$ (full line) and projected densities (dotted lines) for extended s-wave $N_s(E)$ and d-wave type $N_d(E)$; b) $N(E)$ (full line) and p-wave type $N_p(E)$ (dotted line) for a normal pure system, the chemical potential is $\mu = 0$

To calculate the above densities of states we have used the recursion method described in the Appendix A. The appropriate densities of states for the clean system $N(E)$, $N_s(E)$ $N_d(E)$ are plotted in Fig. 3a. Figure 3b shows the projected density for the p-wave $N_p(E)$ in comparison to $N(E)$.

The full line in Fig. 3a corresponds to the electron density of states $N(E)$ with the spectral dependence of $\epsilon_{\mathbf{k}}$ (Eq. (4)) and $t' = 0.45$. The position of the central Van Hove singularity $E_v = -1.8t$ (Fig. 2) corresponds to a band filling of $n = 0.467$. Apart from that singularity one can see another sharp peak in the lower edge of the band and a much smoother one in the upper edge. Both of them are singularities of band edges: bottom and top respectively. For the on-site interaction U_{ii} the shape of $N(E)$ in Fig. 3a and the gap equation (Eq. (15)) indicates that the critical temperature T_c should be enhanced effectively around the first two singularities for relatively low electron densities $n < 1$. As a matter of fact such a situation can be seen in the calculations of T_c (Fig. 4, clean system for curves denoted by '1'). The critical temperature T_c obtained from the Eqs. (19) and (20) for various symmetries of the order parameter are depicted in Fig. 4a–c by lines denoted by '1' as a function of band the filling n. Figure 4a corresponds to extended s-, d-wave cases while Fig. 4b shows T_c for the p-wave solution. In this case a maximum exists in the projected density of states $N_p(E)$ close to the Van Hove singularities in $N(E)$ but it is not so sharp as in $N(E)$ or $N_s(E)$ and $N_d(E)$ because of the additional smearing term $2(\sin k_x a)^2$ in the formula for $N_p(E)$ (Eq. (20)). Nevertheless, this secondary peak also produces the enhancement of the critical temperature T_c (Fig. 4b). For comparison, in Fig. 4c we present T_c for an isotropic on-site s-wave solution. Clearly, these calculations support the Van Hove singularity scenario. Note that at a relatively low temperature the Van Hove singularity is passing $n = 0.467$ (Figs. 2, 3a). The lack of the particle-hole symmetry results in the shift of the maximum value of T_c to a higher value of electron densities so in the optimal doping the superconductor is a hole superconductor.

Moreover for $n \to 2$ we observe the degradation of the critical temperature T_c. In in this limit of slowly changing density of states we can apply the result for the constant density of states

$$N(E) = \frac{1}{D}\,\Theta(E - D/2)\,\Theta(-E + D/2)\,, \tag{21}$$

where D denotes the bandwidth and $\Theta(E)$ is the Heaviside step function.

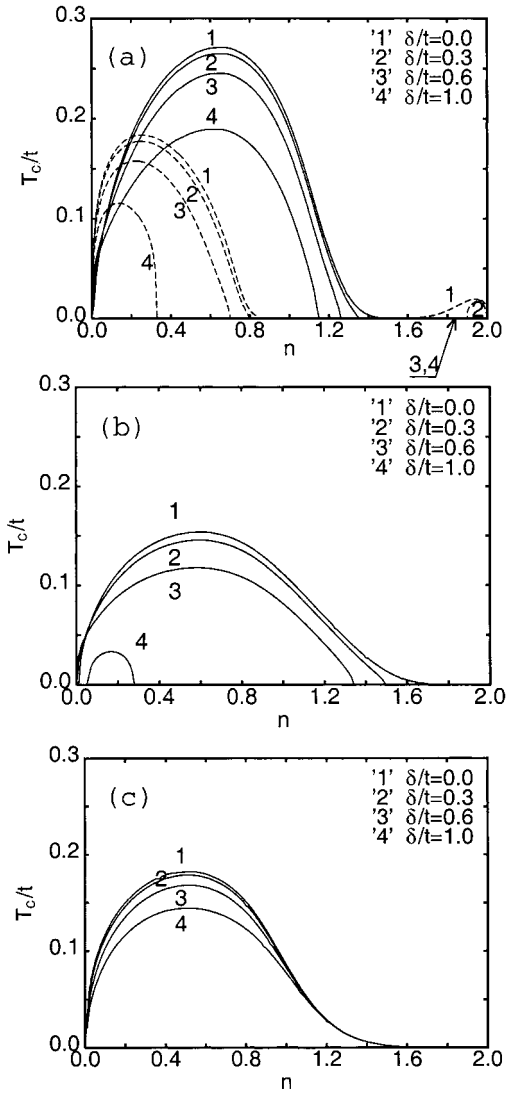

Fig. 4. a) Critical temperature T_c versus band filling n for extended s-wave and d-wave pairing for a pure '1' and alloyed disordered system '2'–'4' (depending on δ); and $U = -1.5t$. Full lines correspond to the d-wave solution and dashed ones to the extended s-wave; b) T_c versus band filling n for the p-wave solution; c) for comparison $T_c(n)$ for the on-site s-wave solution

For small on-site attractive interaction U, the critical temperature T_c^* is given by the analytic formula [68, 70]

$$T_c^* = \frac{e^\gamma}{\pi}\sqrt{n(2-n)}\exp\left(-\frac{D}{|U|}\right). \quad (22)$$

In our case, the degradation of T_c is faster, $T_c \ll T_c{}^*$, due to the asymmetry of the electron density of states $N(E_F) \ll 1/D$ for $n \to 2$.

The Van Hove singularities in the spectrum $\epsilon_{\mathbf{k}}$ show up also in the projected densities of states $N_s(E)$, $N_d(E)$ (Fig. 3a). Due to the factors $\gamma_{\mathbf{k}}$ and $\eta_{\mathbf{k}}$ (Eqs. (17) and (22)) the dependences $T_c(n)$ are severely modified (Fig. 4a, curve '1'). Moreover, the maximum value of $N_p(E)$ (Fig. 3b) is also close to the Van Hove singularity and it results in the optimum of T_c (Fig. 4b, curve '1').

It is worthwhile to notice here that singularities at the band edges are important for an extended s-wave case while the saddle point, located in the middle of the band, is important for d-wave pairing, similarly to an isotropic s-wave case.

The positions of the Van Hove singularities result in the strong band filling n dependence of T_c (Fig. 2b). Again the pairing dominates selected regions of n. In the case of a d-wave it is the middle region of $n \approx 0.5$ while for extended s-wave pairing it is rather the low electron densities region ($n \to 0$); the high electron densities region ($n \to 2$) is also possible, but the T_c is much smaller. The same relation as in the on-site pairing case governs the basic behaviour (Eq. (22)). However, $N(E) = 1/D$ should be substituted by the corresponding projected density of states $N_\alpha(E_F)$. Thus, away the Van Hove singularity ($n \to 2$)

$$T_c^\alpha \approx \exp\left(-\frac{1}{N_\alpha(E_F)|U|}\right) \qquad \alpha = s, p, d\,. \quad (23)$$

In all cases the Van Hove singularities play the mayor role and could be identified as the source of a raise of the critical temperature T_c. Its dependence on doping n should be described rather by a strongly changing function in contrast to the case of a constant density of states (Eq. (14)) where T_c is simply $\sqrt{n(2-n)}$.

However it is also worthwhile to note that depending on the pairing symmetry different Van Hove singularities can matter and because of the nonsymmetric character of densities of states this effect is approximate. Due to this asymmetry we observe the additional shift of the optimal doping towards the center of a band. Interestingly, different Van Hove singularities and corresponding shifts depend on the solution type and the interaction range. Eventually, an extended s-wave solution appears to be an electron superconductor while a d-wave can be identified as a hole one.

The formulae for a critical temperature T_c (Eq. (19)) are based on the integral over the appropriate DOS which possesses Van Hove singularities. The effect of shift is stronger for smaller T_c where a hyperbolic tangent is smearing the function under integrals. It is also worth to note that the Van Hove scenario is working better for superconductors with relatively small transition temperature T_c (which corresponds to a small interaction parameter U). This can easily be seen from the following function

$$F(T_c, E) = \frac{2T_c}{(E-\mu)} \tanh\left(\frac{E-\mu}{2T_c}\right) \tag{24}$$

present in the gap Eqs. (9), (12). It can be interpreted as leading to a natural cut-off E_C around the chemical potential μ. Note that if the temperature T_c is small then the function $F(T_c, E-\mu)$ is not zero in the narrow range of energies around μ only. In fact in the limit $T_c \to 0$ it tends to the Dirac delta function ($F(T_c, E-\mu) \to \delta(E-\mu)$) and the cut-off is limited to the neighbourhood of the $E=\mu$ point. Note, that for finite T_c, $E_C \approx 2T_c$. Consequently, for the logarithmic Van Hove singularity in the density of states near μ it is

$$N(E) \approx -N_0 \ln\left|\frac{E-\mu}{D}\right|, \tag{25}$$

and we get the Labbe-Bok formula for T_c [55, 56, 58]

$$T_c \sim \exp\left\{-\frac{1}{\sqrt{|N_0 U|}}\right\}. \tag{26}$$

3. CPA for the Disordered Hubbard Model

As mentioned above, the technical question we shall answer in this paper is what happens to the above behaviour when the site energies ε_i are not the same on all sites but are randomly distributed. For example in a binary alloy, A_cB_{1-c}, we have random distribution of site energies: $\varepsilon_i = (\varepsilon_A, \varepsilon_B)$ depending on occupation at the site i by atom A or B with probabilities $P_{A,(B)} = c$ and $(1-c)$, respectively. Such a problem has been dealt with on a number of occasions in the past [18–20, 34, 73–78] in the Coherent Potential Approximation (CPA). Here we shall follow the usual arguments generalized as appropriate. In short, we shall take the CPA to mean that the coherent potential $\mathbf{\Sigma}(E) = \mathbf{\Sigma}(i, i; E)$ [72], in a site approximation, is defined by the zero value of an aver-

aged t-matrix $\mathbf{T}(i,i;E)$. Namely

$$\begin{aligned}\langle \mathbf{T}_\alpha(i,i;E)\rangle &= \sum_\alpha P_\alpha \mathbf{T}_\alpha(i,i;E) \\ &= \langle (\mathbf{V}_\alpha - \mathbf{\Sigma}^\sigma(E))\,(\mathbf{1} - [\mathbf{V}_\alpha - \mathbf{\Sigma}(E)]\,\bar{\mathbf{G}}(i,i;E))^{-1}\rangle = 0\,,\end{aligned} \tag{27}$$

where $\alpha = \mathrm{A},\mathrm{B}$ specifies the occupation of the site i and hence the disordered potential $\mathbf{V}_\alpha$.

In case of on-site attraction (Eq. (1) with $U_{ij} = U_{ii}\delta_{ij}$). In the limit of small fluctuations in the pairing potential ($\Delta_{ii} = \Delta_i$), a constant averaged value

$$\Delta_i \to \bar{\Delta} \quad \text{for all } i \tag{28}$$

can be applied.

Using now CPA equations (Eq. (27) and Appendix B) it can be readily shown that due to the disorder $\bar{\Delta}$ and E in the clean limit is renormalized to $\tilde{\Delta}$ and $\tilde{E}$ in the same way

$$\begin{aligned}\tilde{\Delta}(E) &= \bar{\Delta}\,\frac{2E - \operatorname{Tr}\mathbf{\Sigma}(E))}{2E}\,, \\ \tilde{E} &= E\,\frac{2E - \operatorname{Tr}\mathbf{\Sigma}(E))}{2E}.\end{aligned} \tag{29}$$

On account of the general symmetry between the averaged Green function $\mathbf{G}(i,i;E)$ elements and that of the coherent potential $\mathbf{\Sigma}(E)$, for complex energies, it follows that

$$G_{11}(i,j;E) = G_{22}(i,j;-E^*)\,, \tag{30}$$

$$\Sigma_{11}(E) = \Sigma_{22}(-E^*)\,. \tag{31}$$

Note that one can write Eq. (29) in terms of Matsubara frequencies ($E = \mathrm{i}\omega_n$)

$$\frac{\tilde{\Delta}(\omega_n)}{\bar{\Delta}} = \frac{\tilde{\omega}_n}{\omega_n}\,, \tag{32}$$

where

$$\mathrm{i}\tilde{\omega}_n = \mathrm{i}\omega_n - \Sigma_{11}(\mathrm{i}\omega_n)\,. \tag{33}$$

Eventually Eq. (31) leads to the linearized gap equation (Appendix B)

$$1 = U \int_{-\infty}^{\infty} \mathrm{d}E\,\bar{N}(E)\,\frac{\tanh\left(\dfrac{\beta E}{2}\right)}{2E}\,. \tag{34}$$

This equation is related directly to the similar one of the clean case (Eq. (15)) with one difference due to the substitution of the density of states for the pure system $N(E)$ by the averaged one for the doped material $\bar{N}(E)$. Evidently, assuming small fluctuations in the the pairing potential (Eq. (28)) one gets a critical temperature T_c weakly depending on disorder. This is the content of the Anderson theorem [3, 79] which rests on the assumption that the pairing potential does not fluctuate in space $\Delta_i \approx \bar{\Delta}$ for all i. However, it should be noted that in a short coherence length limit the situation can be opposite. In that case, allowing the spatial fluctuations of the pairing amplitude $\Delta_i \neq \Delta_j$

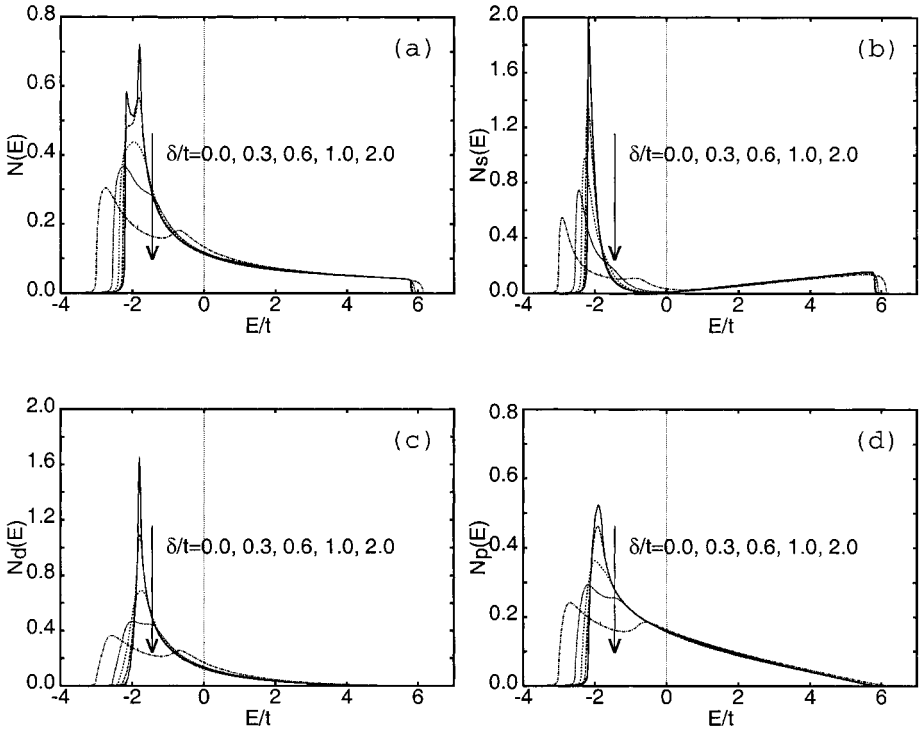

Fig. 5. a) Normal state density of states $N(E)$ and projected densities: b) extended s-wave $N_s(E)$, c) d-wave type $N_d(E)$ and d) p-wave $N_p(E)$, respectively, for different values of disorder strength $\delta/t = 0.0$, 0.1, 0.2, 0.3. Arrows show the directions of δ change. Here, the chemical potential is $\mu = 0$

induced by the site energy disorder $\varepsilon_i \neq \varepsilon_j$ or introduced by the randomly distributed attractive centers ($U_{ii} = 0$ for some lattice sites i), the Anderson theorem breaks down even for conventional on-site s-wave superconductors [77, 78].

For a constant pairing parameter as in Eq. (28) the generic consequence of disorder in the system with on-site attraction is the smearing of the structure in the averaged density of states $\bar{N}(E)$ (Eq. (34)). To illustrate the consequences of it in our model we have calculated $\bar{N}(E)$ using the standard CPA procedure [19, 20, 76] for $c = 0.5$, $\varepsilon_A = -\dfrac{\delta}{2}$, $\varepsilon_B = \dfrac{\delta}{2}$.

The results for various values of the scattering strength δ leading to the smearing of the Van Hove singularities in the averaged density of states $\bar{N}(E)$, are shown in Fig. 5a. Van Hove singularities are still present here for a relatively weak disorder strength $\delta \leq 1t$ while for a stronger one ($\delta = 2t$) one can notice additional splitting of singularities caused by the model of disorder. This is the so called split band regime [72, 78]. Namely the two peaks are the remnant of the Van Hove singularities of the two, A and B, pure metals.

Let us now examine a disordered system with the inter-site attraction U_{ij}. Here we assume that the inter-site pairing parameter Δ_{ij} can be substituted by its average $\bar{\Delta}_{ij}$ [18–20]. Thus, in the case of a singlet pairing (extended s- or d-wave), the on-site im-

purity potential $\mathbf{V}_\alpha$ can be expressed as

$$\mathbf{V}_\alpha = \begin{bmatrix} \varepsilon_\alpha & 0 \\ 0 & -\varepsilon_\alpha \end{bmatrix}; \qquad \alpha = \mathrm{A} \quad \text{or} \quad \mathrm{B}\,, \tag{35}$$

while the coherent potential matrix has the form

$$\mathbf{\Sigma}(E) = \begin{bmatrix} \Sigma_{11}(E) & 0 \\ 0 & \Sigma_{22}(E) \end{bmatrix}. \tag{36}$$

Naturally, the averaged Green function, $\bar{\mathbf{G}}(i,i;E)$ can be expressed as follows:

$$\bar{\mathbf{G}}(i,i;E) = \frac{1}{N}\sum_{\mathbf{k}} \bar{\mathbf{G}}(\mathbf{k};E) = \frac{1}{N}\sum_{\mathbf{k}} \begin{bmatrix} E-\epsilon_{\mathbf{k}}-\Sigma_{11}(E) & \bar{\Delta}_{\mathbf{k}} \\ \bar{\Delta}^*_{\mathbf{k}} & E+\epsilon_{\mathbf{k}}-\Sigma_{22}(E) \end{bmatrix}^{-1}. \tag{37}$$

In case of triplet pairing (p-wave) the following notation should be introduced [34, 35] instead of the Eqs. (35)–(37):

$$\mathbf{V}_\alpha = \begin{bmatrix} \varepsilon_\alpha & 0 & 0 & 0 \\ 0 & \varepsilon_\alpha & 0 & 0 \\ 0 & 0 & -\varepsilon_\alpha & 0 \\ 0 & 0 & 0 & -\varepsilon_\alpha \end{bmatrix}; \qquad \alpha = \mathrm{A} \quad \text{or} \quad \mathrm{B}\,, \tag{38}$$

for the impurity potential and the coherent potential

$$\mathbf{\Sigma}(E) = \begin{bmatrix} \Sigma_{11}(E) & 0 & 0 & 0 \\ 0 & \Sigma_{11}(E) & 0 & 0 \\ 0 & 0 & \Sigma_{22}(E) & 0 \\ 0 & 0 & 0 & \Sigma_{22}(E) \end{bmatrix}, \tag{39}$$

respectively. Again the averaged Green function is given by

$$\bar{\mathbf{G}}(i,i;E) = \frac{1}{N}\sum_{\mathbf{k}} \bar{\mathbf{G}}(\mathbf{k};E) = \frac{1}{N}\sum_{\mathbf{k}} \begin{bmatrix} (E-\epsilon_{\mathbf{k}}-\Sigma_{11}(E))\,\mathbf{1} & \bar{\mathbf{\Delta}}_{\mathbf{k}} \\ \bar{\mathbf{\Delta}}^*_{\mathbf{k}} & (E+\epsilon_{\mathbf{k}}-\Sigma_{22}(E))\,\mathbf{1} \end{bmatrix}^{-1}, \tag{40}$$

while the conditionally averaged Green function at the impurity site ($\alpha = \mathrm{A}$ or B) has the following form:

$$\mathbf{G}_\alpha(i,i;E) = \bar{\mathbf{G}}(i,i;E)\,(\mathbf{1} - [\mathbf{V}_\alpha - \mathbf{\Sigma}_\alpha(E)]\,\bar{\mathbf{G}}(i,i;E))^{-1}. \tag{41}$$

The averaged pairing parameters can be written as in Eqs. (18)

$$\begin{aligned} \bar{\Delta}^{\mathrm{s}}_{\mathbf{k}} &= \bar{\Delta}_0 \gamma_{\mathbf{k}}\,, \\ \bar{\Delta}^{\mathrm{d}}_{\mathbf{k}} &= \bar{\Delta}_0 \eta_{\mathbf{k}}\,, \\ \bar{\mathbf{\Delta}}^{\mathrm{p}}_{\mathbf{k}} &= \bar{\mathbf{\Delta}}^x_0 \sin(k_x a) + \bar{\mathbf{\Delta}}^y_0 \sin(k_y a)\,. \end{aligned} \tag{42}$$

For anisotropic s-, d- and p-wave pairing symmetries the gap equations (Eqs. (9) and (10)) take the form

$$\Delta_{\mathbf{k}} = \frac{1}{N}\sum_{\mathbf{q}} \frac{U_{\mathbf{k}-\mathbf{q}}}{\pi} \int_{-\infty}^{\infty} \mathrm{d}E\, \mathrm{Im}\, \bar{G}_{12}(\mathbf{k};E)\, \frac{1}{\mathrm{e}^{\beta\omega}+1} \tag{43}$$

for singlets (extended s- and d-wave) and

$$\mathbf{\Delta}_{\mathbf{k}} = \frac{1}{N} \sum_{\mathbf{q}} \frac{U_{\mathbf{k}-\mathbf{q}}}{\pi} \int_{-\infty}^{\infty} \mathrm{d}E \, \mathrm{Im} \, \bar{G}_{12}(\mathbf{k}; E) \, \frac{1}{\mathrm{e}^{\beta\omega} + 1} \tag{44}$$

for triplets (p-wave) cases.

From Eqs. (37) and (40) it follows that off-diagonal elements of the Green function are

$$\bar{G}_{12}(\mathbf{k}; E) = \frac{\bar{\mathbf{G}}_{11}(\mathbf{k}; E) + \bar{\mathbf{G}}_{22}(\mathbf{k}; E)}{2E - \Sigma_{11}(E) - \Sigma_{22}(E)} \, \bar{\Delta}_0 \zeta_{\mathbf{k}} \tag{45}$$

for singlets and

$$\bar{\mathbf{G}}_{12}(\mathbf{k}; E) = \frac{\bar{\mathbf{G}}_{11}(\mathbf{k}; E) + \bar{\mathbf{G}}_{22}(\mathbf{k}; E)}{2E - \Sigma_{11}(E) - \Sigma_{22}(E)} \, (\bar{\mathbf{\Delta}}_0^x \sin k_x a + \bar{\mathbf{\Delta}}_0^y \sin k_y a) \tag{46}$$

for triplets, where $\zeta_{\mathbf{k}} = \gamma_{\mathbf{k}}$ or $\eta_{\mathbf{k}}$.

Interestingly, the linearized gap equation can be written in a way similar to that for the clean system (Eq. (19))

$$1 = \frac{|U|}{\pi} \int_{-\infty}^{\infty} \mathrm{d}E \tanh \frac{E\beta_{\mathrm{c}}}{2} \, \mathrm{Im} \, \frac{\bar{G}^{\mathrm{s,d,p}}(E)}{2E - \mathrm{Tr} \, \mathbf{\Sigma} \, (E)} \, . \tag{47}$$

where the imaginary parts of $\bar{G}^{\mathrm{s,d,p}}(E)$ define the projected densities of states for a disordered system $\bar{N}_{\mathrm{s}}(E)$, $\bar{N}_{\mathrm{d}}(E)$ and $\bar{N}_{\mathrm{p}}(E)$ discussed in Appendix A. Moreover, as in the case of a clean system (Eqs. (20))

$$\bar{N}_{\mathrm{s,d,p}}(E) = -\frac{1}{\pi} \, \mathrm{Im} \, \bar{G}^{\mathrm{s,d,p}}(E) = -\frac{1}{\pi N} \sum_{\mathbf{k}} \zeta'_{\mathbf{k}} \, \mathrm{Im} \frac{1}{E - \Sigma_{11}(E) - \varepsilon_{\mathbf{k}} + \mu} \, , \tag{48}$$

where $\zeta'_{\mathbf{k}} = (\gamma_{\mathbf{k}})^2/4, (\eta_{\mathbf{k}})^2/2$ or $2(\sin{(k_x a)})^2$ depending on the symmetry of solution: extended s-, d- and p-wave. Figures 5b–d show the corresponding projected densities of states of a disordered system (Eq. (55)): $\bar{N}_{\mathrm{s}}(E)$, $\bar{N}_{\mathrm{d}}(E)$ and $\bar{N}_{\mathrm{p}}(E)$. Like for $\bar{N}(E)$ (Fig. 5a) for weak disorder, Van Hove singularities survive. Thus, it is clear that the smearing of the Van Hove singularity in Figs. 5a–d implies a weakening of the Van Hove enhancement of the critical temperature T_{c}.

For our simple model of disorder of binary alloy $\mathrm{A}_c\mathrm{B}_{1-c}$ with $c = 0.5$ the coherent potential $\Sigma_{11}(E)$ satisfies the CPA equation [72]:

$$\Sigma_{11}(E) = (\tfrac{1}{2}\delta - \Sigma_{11}(E)) \, \bar{G}_{11}(i, i; E) \, (\tfrac{1}{2}\delta + \Sigma_{11}(E)) \, . \tag{49}$$

In Fig. 6a, b we also show the corresponding self energy $\Sigma(E)$ which in on-site CPA depends only on the energy E but not on the wave vector $\mathbf{k}$. One can see that for a relatively weak disorder strength δ the maximum of $|\mathrm{Im} \, \Sigma_{11}(E)|$ is exactly at the Van Hove singularity as in the Born approximation [12, 19, 20]

$$\mathrm{Im} \, \Sigma(E) \approx -\frac{\pi\delta^2}{4} \, \bar{N}(E) \, . \tag{50}$$

The above result is valid also below the critical temperature T_{c} because for off-diagonal pairing $\Delta_{ii} = 0$ [19, 20] and Eq. (49) is still valid.

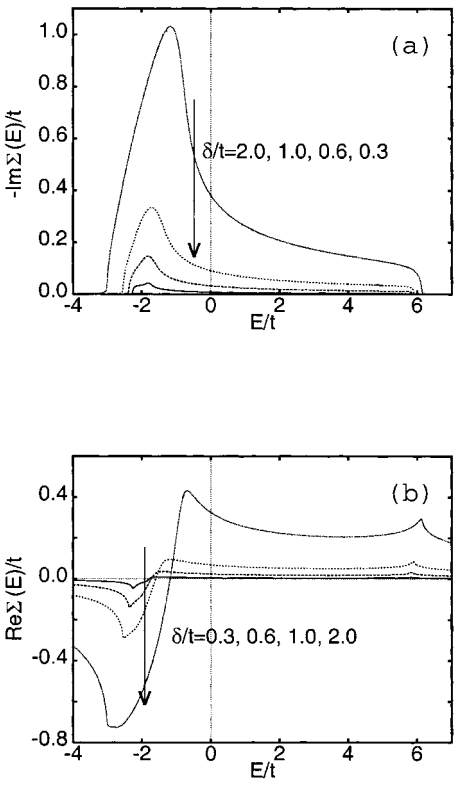

Fig. 6. Normal state parts of self energy $\Sigma(E)$: a) imaginary and b) real for different values of δ

In case of a larger disorder strength δ the maximum of $|\mathrm{Im}\,\Sigma_{11}(E)|$ is located in some other energy according to the model of disorder we use (Eqs. (1), (35)–(41)). Simultaneously the real part of self energy $\mathrm{Re}\,\Sigma_{11}(E)$ is changing with energy E renormalizing the chemical potential μ (Eq. (48)).

Let us investigate the additional effect of disorder visible in Eq. (47). Comparing this equation with the clean system one (Eq. 19) one can notice the difference in the denominator, where in case of disordered system there is an additional strong scattering term $\mathrm{Tr}\,\Sigma(E)$.

To examine it further let us rewrite the gap equation in terms of Matsubara frequencies ω_n

$$1 = \frac{|U|}{\beta_c} \sum_n \mathrm{e}^{\mathrm{i}\omega_n \eta} \frac{\bar{G}^{\mathrm{s,d,p}}(i,i;\mathrm{i}\omega_n)}{\mathrm{i}\omega_n - \Sigma_{11}(\mathrm{i}\omega_n)}\,, \tag{51}$$

for s-, d- and p-wave symmetry.

Now, let us approximate the normal state self energy $\Sigma_{11}(\mathrm{i}\omega_n)$ and projected density of states $\bar{N}_\alpha(\mathrm{i}\omega_n)$ by

$$\Sigma(\mathrm{i}\omega_n) \approx -\mathrm{i}\,|\Sigma_0|\,\mathrm{sgn}\,(\omega_n) \tag{52}$$

$$\begin{aligned}\bar{N}_\alpha(\mathrm{i}\omega_n) &= N_\alpha(\mathrm{i}\omega_n - \Sigma(\mathrm{i}\omega_n)) \approx N(\mathrm{i}\omega_n + \mathrm{i}\,|\Sigma_0|\,\mathrm{sgn}\,(\omega_n)) \\ &= -\frac{1}{\pi}\,\mathrm{Im}\,G^\alpha_{11}(i,i;\mathrm{i}\omega_n + \mathrm{i}\,|\Sigma_0|\,\mathrm{sgn}\,(\omega_n))\,.\end{aligned} \tag{53}$$

In Fig. 7a we have plotted the densities $N^{\mathrm{d}}(\mathrm{i}\omega)$ $N^{\mathrm{p}}(\mathrm{i}\omega)$ $N^{\mathrm{s}}(\mathrm{i}\omega)$ versus the imaginary part of the energy $\mathrm{i}\omega$ for the Fermi energy E_{F} chosen at the Van Hove singularity ($E_{\mathrm{F}} = E_{\mathrm{v}} = 0$).

Note that in that region we can roughly approximate the corresponding projected densities by a simple formula

$$N_\alpha(\mathrm{i}\omega_n) = \frac{a_\alpha}{\omega_n + b_\alpha}\,, \tag{54}$$

where a_α and b_α are constants depending on the pairing symmetry $\alpha =$ s, d, p. Introducing Eq. (54) and Eqs. (52) and (53) into Eq. (51) we get

$$1 = |U|\,a_\alpha T_c \sum_{\omega_n > 0} \frac{2}{\omega_n + \Sigma_0}\,\frac{1}{\omega_n + b_\alpha}\,. \tag{55}$$

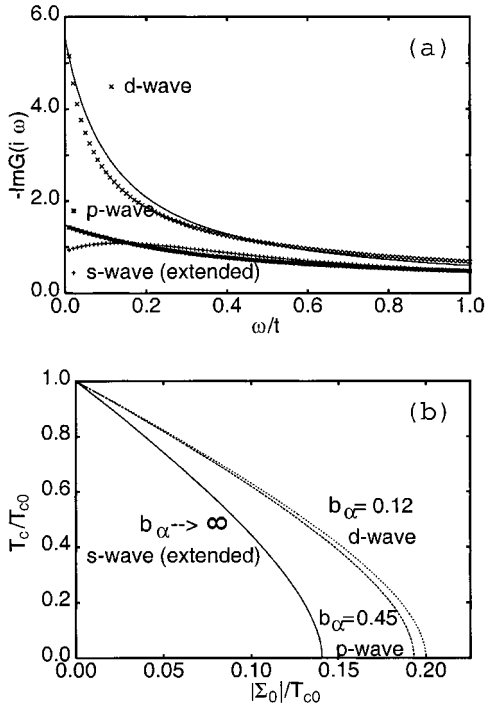

Fig. 7. a) Imaginary part of the Green functions: $-\mathrm{Im}\, G_\mathrm{d}$, $-\mathrm{Im}\, G_\mathrm{p}$ and $-\mathrm{Im}\, G_\mathrm{s}$ versus the imaginary energy $\mathrm{i}\omega$, fitted lines $a_\alpha/(b_\alpha + \omega)$ are plotted for d-wave pairing ($b_\alpha = 0.12$) and p-wave pairing ($b_\alpha = 0.12$), $a_\alpha = 2/3$ for both curves; b) the critical temperature T_c versus the pair breaking parameter $|\Sigma_0|$ in the limit of weak disorder (both T_c and $|\Sigma_0|$ are normalized to $T_{\mathrm{c}0}$ of a clean system) for a few values of b_α. The limit $b_\alpha \to \infty$ corresponds to the standard Abrikosov-Gorkov formula (Eqs. (58)–(59))

Now we have to perform the summation over ω_n for clean ($\Sigma_0 = 0$) and disordered cases ($\Sigma_0 \neq 0$). After some algebra (Appendix C) we get the approximate pair-breaking formula

$$\psi\left(\frac{1}{2}\right) - \psi\left(\frac{1}{2} + \frac{b_\alpha}{2\pi T_{\mathrm{c}0}}\right) = \psi\left(\frac{1}{2} + \frac{\Sigma_0}{2\pi T_\mathrm{c}}\right) - \psi\left(\frac{1}{2} + \frac{\Sigma_0}{2\pi T_\mathrm{c}} + \frac{b_\alpha}{2\pi T_\mathrm{c}}\right), \qquad (56)$$

Note that in the limit the constant density of states $N_\alpha(\mathrm{i}\omega) = \text{const.}$ (Eq. 54), $b_\alpha \to \infty$, we get automatically the the standard Abrikosov-Gorkov formula [3] with a characteristic pair-breaking parameter $\rho_\mathrm{c} = |\mathrm{Im}\, \Sigma_0|/(2\pi T_\mathrm{c})$,

$$\ln\left(\frac{T_\mathrm{c}}{T_{\mathrm{c}0}}\right) = \psi\left(\frac{1}{2}\right) - \psi\left(\frac{1}{2} + \rho_\mathrm{c}\right). \qquad (57)$$

In Eqs. (64) and (65) $T_{\mathrm{c}0}$ denotes the critical temperature in a clean system, while T_c is the critical temperature in a dirty one.

In Fig. 7b we plot $T_\mathrm{c}/T_{\mathrm{c}0}$ versus $\Sigma_0/(2\pi T_{\mathrm{c}0})$ for a few values of b_α. Here the chemical potential μ was fixed at the saddle point Van Hove singularity $E_{\mathrm{v}1}$. Interestingly, the slope of the curve (Fig. 7b) is increasing with decreasing b_α indicating that in the presence of Van Hove singularities for a disordered system we get weaker decreasing of T_c than for a flat density of states. Thus, for d-wave pairing $b_\alpha = 0.12$ and for p-wave $b_\alpha = 0.45$ the superconducting phase is more stable than in the case of extended s-wave pairing, where $b_\alpha \to \infty$ (Fig. 7a). This is the main result obtained in this section. In spite of very rough approximation used here the results show that the Van Hove singularity influences the pair-breaking effect. Namely increasing the critical strength of disorder Σ_0 needed to break the Cooper pairs makes superconductivity more robust.

4. Critical Temperature for Disordered Superconductors

Let us now turn to the case where both superconductivity and disorder are present [73–76] and calculate the critical temperature T_c self-consistently. Although the full CPA program can be implemented for the problem defined by Eqs. (9), (10) and

(B.1)–(B.4) [76, 78] and the specification of the site energy ensemble, it is convenient to make the approximation, valid when the coherence length ξ_0 is much larger then the lattice spacing, that the pairing potential Δ_{ij} does not fluctuate very much and replace it in Eqs. (3) and (5) by its average value $\bar{\Delta}_{ij}$ [79]. For conventional isotopic s-wave pairing the gap equation at T_c takes the simple form (Eq. (34)). Thus, the critical temperature T_c at the optimal doping should be only slightly reduced by disorder due to smearing of the density of states $\bar{N}(E)$. The results of numerical calculations for four different values of the disorder strength δ in case of the on-site attraction is presented in Fig. 4c. Clearly, in this case the critical temperature T_c is slightly reduced by the effect of the density of states.

On the other hand, for the off-diagonal attraction case the linearized gap equation, in presence of disorder, is given by Eq. (57). Solving it for extended s-, d- and p-wave pairing symmetries we get the critical temperature T_c versus band filling. The results for various δ are presented in Fig. 4a (extended s- and d-wave) and Fig. 4b (p-wave). Here, we observe significant degradation of T_c in all three anisotropic pairing cases. Moreover, in some regions of electron concentration, disappearing of a superconducting phase can be noticed for relatively weak disorder ($\delta \leq 0.6t$). Especially this happens to the s-wave case with high electron concentration $n \to 2$ and $n \approx 0.8$ as well as the d-wave case for $n \approx 1.2$ (Fig. 4a). The dramatic degradation of extended s-wave superconductivity for $n > 0.3$ can also be seen for stronger disorder ($\delta = 1t$). In that region of electron concentration n, due to the binary alloy model of disorder A_cB_{1-c} and $c = 0.5$, the position of energy E for the maximum of the pair-breaking term $|\mathrm{Im}\,\Sigma_{11}(E)| \approx \Sigma_0$ (Fig. 6) coincides with the chemical potential μ making the pair-breaking mechanism very efficient. Similar behaviour can be seen for p-wave superconductor (Fig. 4b). Clearly, for large enough $|\mathrm{Im}\,\Sigma_{11}(E)|$ (Figs. 4a, b) the superconductivity is destroyed by the pair-breaking effect shrinking the region of n for $T_c > 0$. In the same time the corresponding projected densities are not strongly affected (Fig. 5). The results for anisotropic pairing in Figs. 4a, b are contrasting with Fig. 4c where we plotted the results for the on-site solution with $U = U_{ii}$. Here, (Fig. 4c) the region of band filling n, where a superconducting solution exists, does not change with disorder at all.

5. Conclusions and Remarks

We have analyzed the effect of disorder on the disordered Hubbard model with local and non-local nearest neighbour interactions as well as nearest and next neighbour electron hopping terms. We have got numerical and analytical results confirming previous works on the similar model with a simple band energy [19, 20] $\epsilon_{\mathbf{k}} = -2t(\cos k_x a + \cos k_y a)$. Such a dispersion relation introduces the electron-hole symmetry for a half filled band $n = 1$ and locates the saddle point Van Hove singularity exactly in the center of the band (Figs. 1a, b). Including the additional hopping t' we break the electron–hole symmetry in the densities of states, resulting in shifting the central Van Hove saddle point singularity to the bottom of the band. In the same time another Van Hove singularity, located at the bottom band edge, appears to be important. Thus, the effect of the Fermi surface distortion makes place both of singularities very close to each other. For some of the band filling values $n \approx 0.4$ both singularities play important roles. It is clear after analyzing the appropriate projected densities of states N_α. Moreover various pairing symmetries choose different Van Hove singulari-

ties. The d-wave symmetry is favored in case of the regions of band fillings n with chemical potential μ near the saddle point singularity E_v while extended s-wave pairing symmetry is more likely as far as the bottom edge singularity is concerned. Interestingly, on account of the non-symmetricity of electron density of states the Van Hove scenario is fulfilled only approximately. Here we observe a small interaction dependent shift of the optimal doping electron concentration $n \approx n_{op}$ towards the center of the band. As a result of the above we conclude that the Van Hove singularity is important for all discussed symmetries of the order parameter. Interestingly, in presence of an additional electron hopping to the next nieghbour lattice site t', the shift of the saddle point Van Hove singularity in the density of states explains that the superconductor with an extended s-wave symmetry is rather of the electron type and with a d-wave symmetry of hole nature. Note also that the positions of the maximum value of $\bar{N}_s(E)$, $\bar{N}_d(E)$, $\bar{N}_p(E)$ (Fig. 5) are not affected by small disorder. Nevertheless small density of states effects are leading to smearing peaks in the corresponding densities: $\bar{N}_s(E)$, $\bar{N}_d(E)$ and $\bar{N}_p(E)$ (Eq. (48), Fig. 5), the critical temperature T_c, plotted in Figs. 4a–b, is degradated strongly with disorder. This is due to the pair-breaking term $\Sigma_{11}(\omega_n)$ (Eq. (51)). In the negative U on-site interaction there is a quite different situation. Here disorder causes only a small decrease of T_c (Fig. 4a) via a density of states effect (Fig. 5a). So, the most interesting effect arises from the Eqs. (51) and (55), where $\Sigma_{11}(E)$ acts as a pair breaker.

Concluding our results we would like to stress that the Van Hove singularity does not make the decrease in T_c more pronounced than expected (because singularities are present in the self-energy $\mathrm{Im}\,\Sigma_{11}(E) \sim N(E)$, Fig. 6). In fact singularities make it weaker. We have analyzed this effect very carefully in Section 3, finding an approximate pair-breaking formula (Eq. (56)). Here, the Van Hove singularity influenced the pair-breaking Abrikosov-Gorkov curve, changing its slope of the T_c versus Σ_0. A similar effect has been observed in the experimental results for Zn-doped LSCO [49]. Alternatively this effect can be also explained assuming anisotropic scattering potentials [6, 7].

Finally, we observed the dependence of T_c on band filling n. Our results for d-wave superconductor show that the Van Hove scenario is valid even in the presence of weak disorder (Fig. 4). Similar experimental results were obtained by measuring T_c in various cuprate compounds as a function of hole concentration, where Cu were substituted by Zn [41, 42]. The concentration of Zn was there the measure of disorder.

However it should be noted that high T_c cuprates are strongly correlated electron systems and the mean field approach, basing on the effective intersite attraction U_{ij} presented here, has a limited applicability [69]. Strictly speaking a more realistic model should possess a strong Coulomb repulsion term, besides an intersite attraction. Although the approximations we used in the present paper aimed to explain the effect of the Van Hove singularity in the presence of disorder in a weak coupling regime, the preliminary calculations using simultaneously slave boson technique and CPA [81] seams to support the general arguments of the Van Hove singularities significance for superconducting cuprates conjectured here.

Appendix A

In this appendix we apply the recursion method to calculate the appropriate densities of the states. Let us investigate the projected densities of the states $N_s(E)$, $N_d(E)$,

$N_{\mathrm{p}}(E)$ and the corresponding Green functions, $\bar{G}^{\mathrm{s}}(E)$, $\bar{G}^{\mathrm{d}}(E)$ and $\bar{G}^{\mathrm{p}}(E)$,

$$\begin{aligned} N_{\mathrm{s}}(E) &= -\frac{1}{\pi}\,\mathrm{Im}\,G^{\mathrm{s}}(E) = -\frac{1}{N}\sum_{\mathbf{k}}\frac{\gamma_{\mathbf{k}}^2}{4}\frac{1}{\pi}\,\mathrm{Im}\,G_{11}(\mathbf{k},E)\,, \\ N_{\mathrm{d}}(E) &= -\frac{1}{\pi}\,\mathrm{Im}\,G^{\mathrm{d}}(E) = -\frac{1}{N}\sum_{\mathbf{k}}\frac{\eta_{\mathbf{k}}^2}{4}\frac{1}{\pi}\,\mathrm{Im}\,G_{11}(\mathbf{k},E)\,, \\ N_{\mathrm{p}}(E) &= -\frac{1}{\pi}\,\mathrm{Im}\,G^{\mathrm{p}}(E) = -\frac{1}{N}\sum_{\mathbf{k}}2(\sin k_x)^2\frac{1}{\pi}\,\mathrm{Im}\,G_{11}(\mathbf{k},E)\,, \end{aligned} \tag{A.1}$$

where $\gamma_{\mathbf{k}}$ and $\eta_{\mathbf{k}}$ were defined in Eq. (11).

Noting trigonometric identities

$$\begin{aligned} \frac{\gamma_{\mathbf{k}}^2}{4} &= \frac{1}{2}(\cos 2k_x + \cos 2k_y) + 1 + 2\cos k_x \cos k_y\,, \\ \frac{\eta_{\mathbf{k}}^2}{4} &= \frac{1}{2}(\cos 2k_x + \cos 2k_y) + 1 - 2\cos k_x \cos k_y\,, \\ 2(\sin k_x)^2 &= 1 - \cos 2k_x\,, \end{aligned} \tag{A.2}$$

the Green functions $G^{\mathrm{s}}(E)$, $G^{\mathrm{d}}(E)$ and $G^{\mathrm{p}}(E)$ can be easily found as a combination of diagonal and off-diagonal Green functions $G_{11}(i+\delta i, i+\delta j, E) = G_{\delta i,\,\delta j}(E)$, see the notation in the schematic picture (Fig. 8),

$$\begin{aligned} G^{\mathrm{s}}(E) &= G_{00}(E) + G_{20}(E) + 2G_{11}(E)\,, \\ G^{\mathrm{d}}(E) &= G_{00}(E) + G_{20}(E) - 2G_{11}(E)\,, \\ G^{\mathrm{p}}(E) &= G_{00}(E) - G_{20}(E)\,. \end{aligned} \tag{A.3}$$

Function $G_{00}(E)$, $G_{20}(E)$ and $G_{11}(E)$ have been calculated using the recursion method [19, 20, 80].

The above procedure can also be used to calculate the average of projected densities $\bar{N}_{\mathrm{s}}(E)$, $\bar{N}_{\mathrm{d}}(E)$ and $\bar{N}_{\mathrm{p}}(E)$ as well as the averaged Green functions $\bar{G}^{\mathrm{s}}(E)$, $\bar{G}^{\mathrm{d}}(E)$ and $\bar{G}^{\mathrm{p}}(E)$ can be calculated via substitution E by $E-\Sigma_{11}(E)$, where local $\Sigma_{11}(E) = \Sigma_{11}(i,i,E)$ should be found self-consistently according to CPA conditions (Eqs. (37)–(43)):

$$\begin{aligned} \bar{G}^{\mathrm{s,d,p}}(E) &= G^{\mathrm{s,d,p}}(E - \Sigma_{11}(E)) \\ \bar{N}_{\mathrm{s,d,p}}(E) &= N_{\mathrm{s,d,p}}(E - \Sigma_{11}(E)). \end{aligned} \tag{A.4}$$

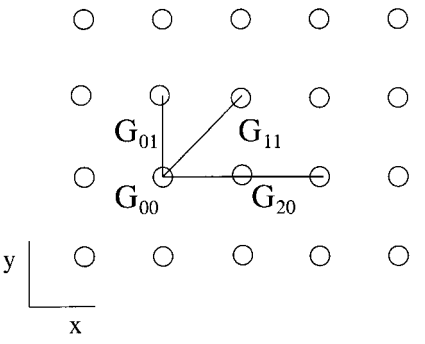

Fig. 8. Schematic picture of diagonal and off-diagonal Green functions $G_{\alpha,\beta} = G(\alpha\hat{\mathbf{x}} + \beta\hat{\mathbf{y}})$

Appendix B

In this appendix we apply CPA equations (Eqs. (18)–(21)) to the disordered Hubbard model with the on-site attraction Eq. (1) ($U_{ij} = U_{ii}\delta_{ij}$) and discuss the Anderson theorem [1, 79]. The averaged Green function, $\bar{\mathbf{G}}(i,i;E)$ can be expressed as

$$\bar{\mathbf{G}}(i,i;E) = \frac{1}{N}\sum_{\mathbf{k}} \bar{\mathbf{G}}(\mathbf{k};E) = \frac{1}{N}\sum_{\mathbf{k}} \begin{bmatrix} E - \epsilon_{\mathbf{k}} - \Sigma_{11}(E) & -\Sigma_{12}(E) \\ -\Sigma_{21}(E) & E + \epsilon_{\mathbf{k}} - \Sigma_{22}(E) \end{bmatrix}^{-1}, \tag{B.1}$$

while the conditionally averaged Green function has the form

$$\mathbf{G}_{\alpha}(i,i;E) = \bar{\mathbf{G}}(i,i;E)\,(\mathbf{1} - [\mathbf{V}_{\alpha} - \mathbf{\Sigma}_{\alpha}(E)]\,\bar{\mathbf{G}}(i,i;E))^{-1}\,. \tag{B.2}$$

The disordered potential in Eq. (18) has the form [76, 77, 78]

$$\mathbf{V}_{\alpha} = \begin{bmatrix} \varepsilon_{\alpha} & -\Delta_{\alpha} \\ -\Delta_{\alpha}^{*} & -\varepsilon_{\alpha} \end{bmatrix}, \tag{B.3}$$

where $\varepsilon_{\alpha} = \varepsilon_{\mathrm{A}}$ or ε_{B} corresponds to different site energies of the lattice site while $\Delta_{\alpha} = \Delta_{\mathrm{A}}$ or Δ_{B} relates to the different pairing potential in an alloy $\mathrm{A}_c B_{1-c}$.

Clearly, the coherent potential can be written as

$$\mathbf{\Sigma}(E) = \begin{bmatrix} \Sigma_{11}(E) & \Sigma_{12}(E) \\ \Sigma_{21}(E) & \Sigma_{22}(E) \end{bmatrix}. \tag{B.4}$$

Function $\bar{G}_{12}(i,i;E)$ can be obtained from Eq. (B.1)

$$\begin{aligned} \bar{G}_{12}(i,i;E) &= \frac{\bar{G}_{11}(i,i;E) + \bar{G}_{22}(i,i;E)}{2E - \Sigma_{11}(E) - \Sigma_{22}(E)}\,\Sigma_{12}(E) \\ &= \left\langle \frac{G^{\alpha}_{11}(i,i;E) + G^{\alpha}_{22}(i,i;E)}{2E - \Sigma_{11}(E) - \Sigma_{22}(E)}\,\Sigma_{12}(E) \right\rangle, \end{aligned} \tag{B.5}$$

while from Eq. (B.4) we have the relations

$$\mathrm{Tr}\,\mathbf{G}^{\alpha}(i,i;E) = \mathrm{Det}\,\mathbf{G}^{\alpha}(i,i;E)\left(\frac{\mathrm{Tr}\,\bar{\mathbf{G}}(i,i;E)}{\mathrm{Det}\,\bar{\mathbf{G}}(i,i;E)} - \mathbf{\Sigma}_{11}(E) - \mathbf{\Sigma}_{22}(E)\right), \tag{B.6}$$

$$G^{\alpha}_{12}(i,i;E) = \mathrm{Det}\,\mathbf{G}^{\alpha}(i,i;E)\left(\frac{\bar{G}_{12}(i,i;E)}{\mathrm{Det}\,\bar{\mathbf{G}}(i,i;E)} - \Delta_{\alpha} - \Sigma_{12}(E)\right). \tag{B.7}$$

The substitution of Eq. (B.6) and (B.7) into the right and left hand sides of Eq. (B.5), respectively, an equation on $\Sigma_{12}(E)$ and Δ_{α} leads to

$$\frac{2E\Sigma_{12}(E)}{2E - \Sigma_{11}(E) - \Sigma_{22}(E)} = \frac{\langle \Delta_{\alpha}\,\mathrm{Det}\,\mathbf{G}^{\alpha}(i,i;E)\rangle}{\langle \mathrm{Det}\,\bar{\mathbf{G}}(i,i;E)\rangle}\,. \tag{B.8}$$

Using (B.6) and factorizing of the equation above we get

$$\frac{2E\Sigma_{12}(E)}{2E - \Sigma_{11}(E) - \Sigma_{22}(E)} \approx \frac{c\,\mathrm{Tr}\,\mathbf{G}^{\mathrm{A}}(i,i;E)\,\Delta^{\mathrm{A}} + (1-c)\,\mathrm{Tr}\,\mathbf{G}^{\mathrm{B}}(i,i;E)\,\Delta^{\mathrm{B}}}{\mathrm{Tr}\,\bar{\mathbf{G}}(i,i;E)}\,. \tag{B.9}$$

In the limit of a small pairing potential fluctuations $\Delta_i \to \bar{\Delta} = \mathrm{const.}$ can be used to satisfy the Anderson theorem. Then

$$\frac{2E\Sigma_{12}(E)}{2E - \Sigma_{11}(E) - \Sigma_{22}(E)} \approx \bar{\Delta} \tag{B.10}$$

and renormalized quantities of ω and $\bar{\Delta}$ read as

$$2\tilde{E} = 2E - \mathrm{Tr}\,\mathbf{\Sigma}(E)\,,$$
$$\tilde{\Delta}(E) = \Sigma_{12}(E) = \frac{(2E - \mathrm{Tr}\,\mathbf{\Sigma}(E))}{2E}\,\bar{\Delta}\,. \tag{B.11}$$

This leads to the same renormalization in the pair potential Δ and energy E

$$\frac{\tilde{\Delta}(E)}{\bar{\Delta}} = \frac{\tilde{E}}{E}\,, \tag{B.12}$$

and the linearized gap equation can be written as follows:

$$\bar{\Delta} = -\frac{U}{\pi}\int_{-\infty}^{\infty} \mathrm{d}E\,\frac{\mathrm{Im}\,(\bar{G}_{11}(E) + \bar{G}_{22}(E))\,\tilde{\Delta}}{2\tilde{E}}\,\frac{1}{\mathrm{e}^{\beta E}+1}$$
$$= -\frac{U}{\pi}\int_{-\infty}^{\infty} \mathrm{d}E\,\frac{\mathrm{Im}\,\bar{G}_{11}(E)\,\bar{\Delta}}{2E}\,\tanh\left(\frac{\beta E}{2}\right), \tag{B.13}$$

$$1 = U\int_{-\infty}^{\infty} \bar{N}(E)\,\mathrm{d}E\,\frac{\tanh\,(\beta_{\mathrm{c}}E)}{2\omega}\,, \tag{B.14}$$

where $N(E)$ denotes normal state DOS:

$$\bar{N}(E) = -\frac{1}{\pi}\,\mathrm{Im}\,G_{11}(E)\,. \tag{B.16}$$

Appendix C

In this appendix we apply CPA to anisotropic superconductor and evaluate the approximate formula of the pair-breaking effect. Starting from the clean system we assume that the linearized gap equation can be written (Eqs. (53)–(57)) as

$$1 = |U|\,a^{\alpha}\pi T_{\mathrm{c}0}\sum_{\omega_n>0}\frac{2}{\omega_n}\,\frac{1}{\omega_n + b_\alpha} \approx \frac{|U|\,a^{\alpha}2\pi T_{\mathrm{c}0}}{b_\alpha}\sum_{\omega_n>0}^{\omega_n^c}\left(\frac{1}{\omega_n} - \frac{1}{\omega_n + b_\alpha}\right), \tag{C.1}$$

where ω_n^c is a cut-off in the summation (C.1). As ω_n^c is very large, it yields

$$\frac{b_\alpha}{|U|a_\alpha} \approx \psi\left(\frac{1}{2}\right) - \psi\left(\frac{1}{2} + \frac{b_\alpha}{2\pi T_{\mathrm{c}0}}\right). \tag{C.2}$$

On the other hand for a disordered system we have

$$1 = |U|\,a^{\alpha}\pi T_{\mathrm{c}}\sum_{\omega_n>0}\frac{2}{\omega_n + |\Sigma_0|}\,\frac{1}{\omega_n + |\Sigma_0| + b_\alpha}$$
$$\approx \frac{|U|\,a^{\alpha}2\pi T_{\mathrm{c}}}{b_\alpha}\sum_{\omega_n>0}^{\omega_n^c}\left(\frac{1}{\omega_n + |\Sigma_0|} - \frac{1}{\omega_n + b_\alpha + |\Sigma_0|}\right). \tag{C.3}$$

Similarly to Eqs. (C.1) and (C.2) it leads to

$$\frac{b_\alpha}{|U|a_\alpha} \approx \psi\left(\frac{1}{2} + \rho_{\mathrm{c}}\right) - \psi\left(\frac{1}{2} + \rho_{\mathrm{c}} + \frac{b_\alpha}{2\pi T_{\mathrm{c}}}\right), \tag{C.4}$$

and finally comparing Eqs. (C.2) and (C.4) we get

$$\psi\left(\frac{1}{2}\right) - \psi\left(\frac{1}{2} + \frac{b_\alpha}{2\pi T_{c0}}\right) = \psi\left(\frac{1}{2} + \rho_c\right) - \psi\left(\frac{1}{2} + \rho_c + \frac{b_\alpha}{2\pi T_c}\right), \tag{C.5}$$

where ρ_c is a pair–breaking parameter

$$\rho_c = \frac{|\Sigma_0|}{2\pi T_c} \tag{C.6}$$

and T_{c0} is the critical temperature for a clean superconductor.

Acknowledgements This work has been partially supported by KBN grant No. 2P03B09018. A part of this work has been done during the stay in the Abdus Salam International Centre for Theoretical Physics in Trieste. The author would like to thank Prof. K. I. Wysokinski, Prof. B. L. Györffy and Dr. J. F. Annett for helpful discussions.

References

[1] P. W. Anderson, J. Phys. Chem. Solids **11**, 26 (1959).
[2] A. A. Abrikosov and L. P. Gorkov, Sov. Phys. – JETP **8**, 1090 (1959).
[3] K. Maki, in: Superconductivity, Vol. 2, Chap. 8, Ed. R. D. Parks, Marcel Dekker, New York 1969.
[4] Y. Sun and K. Maki, Phys. Rev. B **51**, 6059 (1995).
[5] K. Maki and S. Haas, Phys. Rev. B **62**, R11962 (2000).
[6] G. Harań and A. D. Nagi, Phys. Rev. B **58**, 12441 (1998).
[7] G. Harań and A. D. S. Nagi, Phys. Rev. B **63**, 2503 (2001).
[8] D. Belitz and T. R. Kirkpatrick, Rev. Mod. Phys. **66**, 261 (1994).
[9] A. Ghosal, M. Randeria, and N. Trivedi, Phys. Rev. B **63**, 7301 (2001).
[10] J. F. Annett, N. Goldenfeld, and A. J. Leggett, in: Physical Properties of High Temperature Superconductors, Vol. 5, Ed. D. M. Ginsberg, World Scientific, Singapore 1996.
[11] J. F. Annett, Physica C **323**, 146 (1999).
[12] L. P. Gorkov and P. A. Kalugin, JETP Lett. **41**, 253 (1983).
[13] S. V. Pokrovsky and V. L. Pokrovsky, Phys. Rev. B **54**, 13275 (1996).
[14] A. A. Nersesyan, A. M. Tsvelik, and F. Wenger, Phys. Rev. Lett. **72**, 2628 (1994).
[15] A. A. Nersesyan, A. M. Tsvelik, and F. Wenger, Nucl. Phys. B **438**, 561 (1995).
[16] A. A. Nersesyan and A. M. Tsvelik, Phys. Rev. Lett. **78**, 3981 (1997).
[17] R. Fehrenbacher, Phys. Rev. Lett. **77**, 1849 (1996).
[18] F. Wenger, Z. Phys. B **98**, 171 (1995).
[19] G. Litak, A. M. Martin, B. L. Györffy, J. F. Annett, and K. I. Wysokiński, Physica C **309**, 257 (1998).
[20] A. M. Martin, G. Litak, B. L. Györffy, J. F. Annett, and K. I. Wysokiński, Phys. Rev. B **60**, 7523 (1999).
[21] R. J. Radtke, K. Levin, H-B. Schuttler and M. R. Norman, Phys. Rev. B **48**, 15957 (1993).
[22] B. C. Den Hertog and M. P. Das, Phys. Rev. B **58**, 2838 (1998).
[23] L. A. Openov, Pisma Zh. Eksp. Teor. Fiz. **66**, 627 (1997).
[24] L. S. Borkowski and P. J. Hirschfeld, Phys. Rev. B **49**, 15404 (1994).
[25] L. A. Openov, Phys. Rev. B **58**, 9468 (1998).
[26] C. Buhler, S. Yunoki, and A. Moreo, Phys. Rev. B **62**, R3620 (2000).
[27] V. M. Loktev and Yu. G. Pogorelov, cond-mat/0104581.
[28] Y. Maeno, H. Hashimoto, K. Yoshida, S. Nishizaki, T. Fujita, J. G. Bednorz and F. Lichtenberg, Nature **372**, 532 (1994).
[29] G. Baskaran, Physica B **224**, 490 (1996).
[30] D. F. Agterberg, T. M. Rice, and M. Sigrist, Phys. Rev. Lett. **78**, 3374 (1997).
[31] Y. Maeno, T. M. Rice, and M. Sigrist, Phys. Today **54**, 42 (2001).
[32] K. Myake and O. Narikiyo, Phys. Rev. Lett. **83**, 1423 (1999).

[33] E. PUCHKARYOV and K. MAKI, Physica C **341**, 727 (2000).
[34] G. LITAK, J. F. ANNETT, and B. L. GYÖRFFY, Acta Phys. Pol. A **97**, 249 (2000).
[35] G. LITAK, J. F. ANNETT, and B. L. GYÖRFFY, in: Open Problems in Strongly Correlated Electron Systems, Eds. J. BONCA et al., Kluver, Dordrecht 2001 (p. 425).
[36] K. WESTERHOLT and B. VON HEDT, J. Low. Temp. Phys. **95**, 123 (1994).
[37] N. PENG and W. Y. LIANG, Physica C **233**, 61 (1994).
[38] K. UCHINOKURA, T. INO, I. TERESAKI, and TSAKUDA, Physica B **205**, 234 (1995).
[39] E. R. ULM, J. T. KIM, T. R. LEMBERGER, S. R. FOLTYN, and X. D. WU, Phys. Rev. B **51**, 9193 (1995).
[40] G. XIAO, M. Z. CIEPLAK, J. Q. XIAO, and C. L. CHIEN, Phys. Rev. B **43**, 1245 (1990).
[41] C. BERNHARD, J. L. TALLON, C. BUCCI, R. DE RENZI, G. GUIDI, G. V. M. WILLIAMS, and CH. NIEDERMAYER, Phys. Rev. Lett. **77**, 2304 (1996).
[42] J. L. TALLON, C. BERNHARD, G. V. M. WILLIAMS, and J. W. LORAM, Phys. Rev. Lett. **79**, 5294 (1997).
[43] Y. K. KUO, C. W. SCHNEIDER, M. J. SKOVE, M. V. NEVIT, G. X. TESSEMA, and J. J. MCGEE, Phys. Rev. B **56**, 6201 (1997).
[44] G. V. M. WILLIAMS and J. T. TALLON, Phys. Rev. B **57**, 10984 (1998).
[45] J. GIAPINTZAKIS, D. M. GINSBERG, M. A. KIRK, and S. OCKERS, Phys. Rev. B **50**, 15967 (1994).
[46] V. F. ELESIN, K. E. KONKOV, A. V. KRASHENINNIKOV, and L. A. OPENOV, Sov. Phys. — JETP **83**, 395 (1996) [Zh. Eksp. Teor. Fiz. **110**, 731 (1996)].
[47] M. Z. CIEPLAK, K. KARPIŃSKA, J. DOMAGAŁA, E. Dynowska, M. BERKOWSKI, A. MALINOWSKI, S. GUHA, M. CROFT, and P. LINDENFELD, Appl. Phys. Lett. **73**, 2823 (1998).
[48] K. KARPIŃSKA, P.-A. VIEILLEFOND, M. Z. CIEPLAK, F. RULLIER-ALBENQUE, A. MALINOWSKI, and M. BERKOWSKI, Mol. Phys. Rep. **20**, 91 (1997).
[49] K. KARPIŃSKA, M. Z. CIEPLAK, S. GUHA, A. MALINOWSKI, T. SKOŚKIEWICZ, W. PLESIEWICZ, M. BERKOWSKI, B. BOYCE, T. R. LEMBERGER, and P. LIDENFELD, Phys. Rev. Lett. **84**, 155 (2000).
[50] Z. Q. MAO, Y. MORI, and Y. MAENO, Phys. Rev. B **60**, 610 (1999).
[51] R. P. MACENZIE, R. K. W. HASELWIMMER, A. W. TYLER, G. G. LONZARICH, Y. MORI, S. NISHIZAKI, and Y. MAENO, Phys. Rev. Lett. **80**, 161 (1998).
[52] R. S. MARKIEWICZ, J. Phys. Chem. Solids **58**, 1173 (1997).
[53] J. FRIEDEL, J. Phys.: Condens. Matter **1**, 7757 (1989).
[54] I. E. DZIALOSHINSKII, Zh. Eksp. Teor. Fiz. **93** 1487 (1987) [Sov. Phys. – JETP **66** 848 (1987)].
[55] J. LABBÉ and J. BOK, Europhys. Lett. **3**, 1225 (1987).
[56] C. C. TSUEI, D. M. NEWNS, C. C. CHI, and P. C. PATTNAIK, Phys. Rev. Lett. **65**, 2724 (1990).
[57] J. BOK and J. BOUVIER, Physica C **282–287**, 294 (1997).
[58] J. BOUVIER and J. BOK, in: The Gap Symmetry and Fluctuations in High Temperature Superconductors, Eds. J. BOK et al., Plenum, New York 1998.
[59] J. BOK and J. BOUVER, J. Supercond. **13**, 781 (2000).
[60] Z. SZOTEK, B. L. GYÖRFFY, W. M. TEMMERMAN, and O. K. ANDERSEN, Phys. Rev. B **58**, 522 (1998).
[61] O. K. ANDERSEN, O. JEPSEN, and A. I. LIECHTENSTEIN, Phys. Rev. B **49**, 4145 (1994).
[62] D. L. NOVIKOV and A. J. FREEMAN, in: Recent Developments in High Temperature Superconductivity, Eds. J. KLAMUT, B. W. VEAL, B. M. DABROWSKI, P. W. KLAMUT, and M. KAZIMIERSKI, Springer, Berlin 1996.
[63] W. E. PICKETT, Physica C **289**, 51 (1997).
[64] D. M. NEWNS, C. C. TSUEI, and P. C. PATTNAIK, Phys. Rev. B **52**, 13611 (1995).
[65] D. QUESADA, A. RUBIO-PONCE, R. BAQUERO, R. PENA, and C. TRALLERO-GINER, cond-mat/9905081.
[66] D. QUESADA, R. PEÑA, and C. TRALLERO-GINER, Physica C **322**, 169 (1999).
[67] D. H. LU, M. SCHMIDT, T. R. CUMMINS, S. SCHUPPLER, F. LICHTENBERG, and J. G. BEDNORZ, J. Low Temp. Phys. **105**, 1587 (1996).
[68] R. MICNAS, J. RANNINGER, and S. ROBASZKIEWICZ, Rev. Mod. Phys. **62**, 1 (1990).
[69] R. MICNAS and S. ROBASZKIEWICZ, in: High-T_c Superconductivity 1996: Ten Years after the Discovery, Eds. E. KALDIS, E. LIAROKAPIS, and K. A. MÜLLER, Kluwer, Dordrecht 1997 (p. 31).
[70] R. MICNAS, J. RANNINGER, S. ROBASZKIEWICZ, and S. TABOR, Phys. Rev. B **37**, 9410 (1988).
[71] M. TINKHAM, Introduction to Superconductivity, McGraw-Hill, New York 1975.
[72] R. J. ELLIOT, J. A. KRUMHANSL, and P. L. LEATH, Rev. Mod. Phys. **46**, 465 (1974).
[73] H. LUSTFELD, J. Low. Temp. Phys. **12**, 595 (1973).

[74] G. KERKER and K. H. BENNEMANN, Solid State Commun. **14**, 365 (1974).
[75] K. I. WYSOKIŃSKI and A. L. KUZEMSKY, J. Low Temp. Phys. **52**, 81 (1983).
[76] G. LITAK, K. I. WYSOKIŃSKI, R. MICNAS, and S. ROBASZKIEWICZ, Phys. C **199**, 191 (1992).
[77] G. LITAK and B. L. GYÖRFFY, Phys. Rev. B **62**, 6629 (2000).
[78] R. MORADIAN, J. F. ANNETT, B. L. GYÖRFFY, and G. LITAK, Phys. Rev. B **6302**, 4502 (2001).
[79] B. L. GYÖRFFY, G. LITAK, and K. I. WYSOKIŃSKI, in: Fluctuation Phenomena in High Temperature Superconductors, Eds. M. AUSLOOS and A. A. VARLAMOV, Kluwer, Dordrecht 1997 (p. 385).
[80] G. LITAK, P. MILLER, and B. L. GYÖRFFY, Physica C **251**, 263 (1995).
[81] M. KRAWIEC, T. DOMAŃSKI, G. LITAK, and K. I. WYSOKIŃSKI, Mol. Phys. Rep. **34**, 22 (2001).